AN ANTHROPOMETRIC ARM FOR THE HUMANOID ROBOT: DESIGN AND ANALYSIS OF THE TYCHE-ARM

T.C. Yih[§],Madhu. V. Shurpali
Department of Mechanical and Aerospace
Engineering
University of Texas at Arlington
500 West First St., Box 19018
Arlington, TX 76019

Sankar Pemmaraju
Department of Osteopathic Manipulative
Medicine
University of North Texas Health Science Center
Fort Worth, TX 76017

Abstract:

This paper is concerned with the development of an anthropometric robot arm for the humanoid robot – Tyche. The design was based on physiology and anthropometry of the human arm. The Tyche-arm uses a skew-pantograph mechanism, as the control device, that helps in magnifying the input. The link lengths of the structure are determined based on topological studies and avoidance of the singularity condition. A fault tolerant design for the linear actuator is incorporated in the design. The kinematic and dynamic analyses of the Tyche-arm are performed on the weight lifting activity, with the upper arm fixed in five different positions. The kinematic parameters, axial forces in the links and the torques for each joint are obtained and plotted with respect to time.

1. INTRODUCTION

Over the last decade, the field of robotics has expanded and robots are now being designed for medical applications, space exploration, human aides etc. The various aspects of humanoid robots like history, benefits, available technology etc have been described in [1] and [2]. SDR-3, ASIMO, ISAC [3]-[5] are some of the humanoid robots developed. NASA's experimentation with humanoid robots, for space exploration, has led to the development of Robonaut [6]. Robonaut has two arms, two five fingered hands, a head and a torso. ARMAR [7], developed by Berns et al., is a humanoid service robot that consists of two anthropometric arms, a mobile wheel driven platform and

a torso. Mark-2 [8] is an anthropometric arm whose movements are performed at human speeds. It is important to understand the kinematic and dynamic behavior of a robotic system to decide the control strategy of the system. Numerous analytical approaches and algorithms have been developed for performing kinematic and dynamic analyses on a robotic system [9-13]. In this paper the design of the arm of a humanoid robot, Tyche, based on the average anthropometric data of the human body is presented. The first phase of the research involved physiological and anthropometric study of the human arm. The geometries of the links are determined based on topological studies and avoidance of singularity condition. A pantograph mechanism, which serves as mechanical equivalent of bicep, is designed to control the motions of the forearm. The kinematic and dynamic analyses are carried out using software Simulation and Analysis of Mechanism (SAM). The weight lifting activity is simulated and analyzed since maximum forces are generated during such activity. The analyses are carried out with the upper arm fixed at five different configurations. During the analyses the wrist carries a payload of 0 to 40 Kg, varying with a step of 10 Kg.

2. DESIGN OF THE ANTHROPOMETRIC TYCHE-ARM

Prior to the design of the Tyche-arm, the physiology and anthropometry were studied to determine the ranges of motion of upper arm and forearm and to know the various types of motions at the joints.
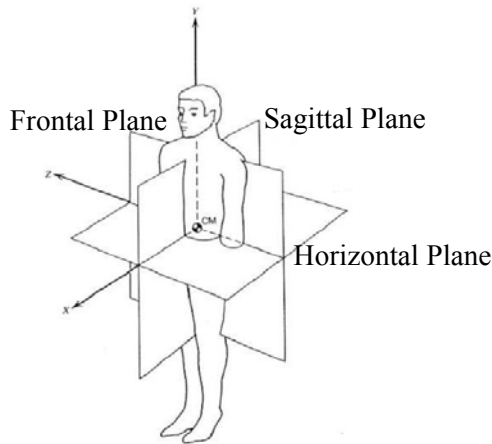
CORRESPONDANCE AUTHOR: T.C.YIH

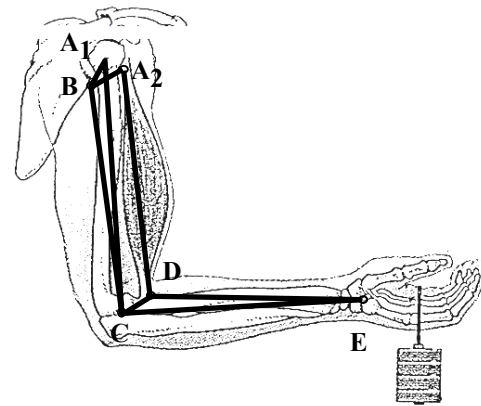Fig. 1 The Three planes used describe human motions

Fig. 2 Conceptual design of the Tyche-arm

2.1 Physiology and Anthropometry of Human Arm

The human arm consists of three joints, the shoulder, the elbow and the wrist, and is made up of upper arm and forearm. The shoulder joint has three degrees of freedom, making it possible for the arm to move in three planes. Fig. 1 shows the three planes used to describe the human motions: sagittal plane, frontal plane, and transverse (horizontal) plane [14]. The upper arm has a range of -50° to 180° in the sagittal plane. The reference position is obtained when the arm hangs vertically by the side of trunk. Movements of the upper arm in sagittal plane are termed as flexion and extension. Flexion is defined as forward motion of the limb; a backward movement is called extension.

The forearm has a range of 0° to 145°. The reference position for the forearm is obtained when the shoulder, elbow and the wrist are collinear.

2.2 Conceptual Design of the Tyche-arm

Fig 2 shows the conceptual design of the Tyche-arm super-imposed on the human arm. A_1, C and E are at shoulder, elbow and wrist respectively. The Tyche-arm structure consists of two ternary links A_1BC and CDE, which constitute the upper arm and forearm respectively. As shown in the figure the bicep is replaced by the links A_2B and A_2D that connect A_1BC and CDE. These two links form a part of the parallelogram A_2BCD and are considered the mechanical equivalence of the bicep. B, A_2, C, D, E are all revolute joints. The anatomical complexity of the shoulder presents a challenge while designing the shoulder joint. The shoulder joint, A_1, consists of two consecutive revolute joints with the joint axis perpendicular to each other – similar to the hook joint. The structure of Tyche-arm is nothing but a skew

pantograph. A pantograph has the advantage of magnified output and higher precision.

2.3 Final Design based on Topological study

The final design is based on average anthropometric data and singularity condition avoidance.

2.3.1 Topological Study

Since A_1C and CE represent the upper arm and forearm respectively, their lengths are calculated based on the average anthropometric data, which provides the average lengths of human body segment as a ratio [15] of body

Table 1. Average anthropometric data

Segment	Link	H−Ratio (Length)
Upper arm	A_1C	0.186H(31.62 cm)
Forearm	CE	0.146H(24.65 cm)
Hand	(Designed separately)	0.108H(18.36 cm)
Thoracic	-	0.189H(32.13 cm)
Lumbar + Sacrum		0.099H(16.83 cm)

height (H), Table 1. The average body height of 170 cm is used for calculating the link lengths. The link lengths of A_1C and CE are then used to determine the geometry of the ternary links. The fully flexed – Fig. 3a and fully extended – Fig. 3b positions of the forearm are used to calculate the link lengths of other links. It is assumed that at full extension of the forearm (forearm at 0° with respect to the upper arm) the joints B, A_2, C and D are collinear. Thus referring to Fig. 3a and 3b it can be concluded that $\angle A_2BC = 145°$. Define $\angle BA_1C$ and $\angle A_1BA_2$ as β_1 and β_2 respectively in ΔA_1BC:
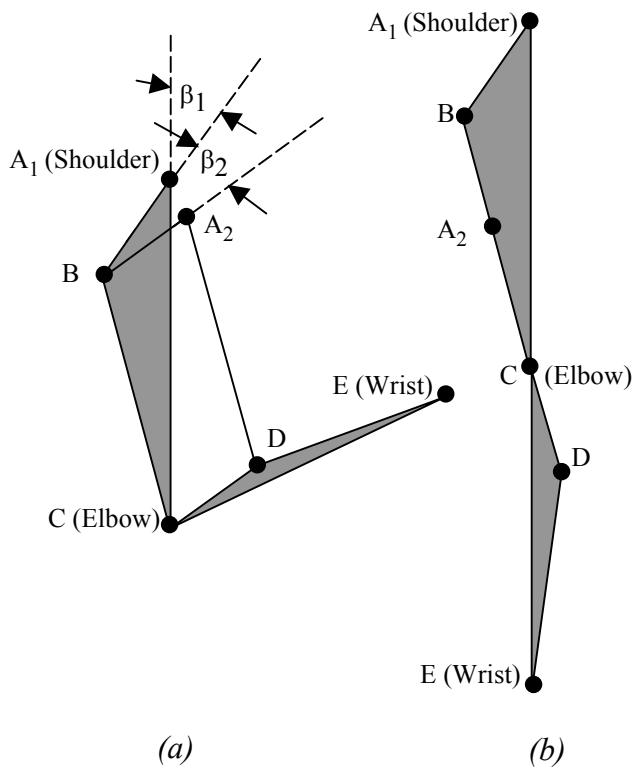
2   Copyright © 2002 ARDC by ASME

Fig. 3 The pantograph mechanism considered
for the Tyche-arm

(a) Forearm in fully flexed position

(b) Forearm in fully extended position

$$\angle A_1BC + \angle BCA_1 + \angle CA_1B = 180$$

that is $(145 + \beta_2) + \angle BCA_1 + \beta_1 = 180$

$$\angle BCA_1 = 35 - (\beta_1 + \beta_2)$$

thus $\beta_1 + \beta_2 \leq 35°$ (1)

Based on the constraint stated above, topological study of the Tyche-arm is performed by varying β_1 and β_2 and by assuming different positions of the joint A_2 at the fully flexed position of the upper limb. First it is assumed that A_2 is aligned with A_1C when the forearm is in full flexion. There are four topologies generated while varying β_1 and β_2 with combinations of 10° and 15°. Larger values of β_1 are not considered since that would mean increasing the length of sides of the ternary links. Thus increasing the weight of the links. The link lengths of A_1B, BC, CD and DE as well as angles $\angle A_1BC$ and $\angle CDE$ for each case are tabulated in Table 2. To select the most appropriate design of the four cases, the area of ternary links A_1BC and CDE are considered. Larger area of the two links would mean more weight of the links and thus a larger actuator would be needed for actuation. Of all the four cases in Table 2, links A_1BC and CDE of

Case 4 have the least area, also the parallelogram mechanism of this Case has least volume hence needing a smaller work volume during its working.

Four more topologies are generated when the A_1B and A_2B are assumed to be equal and β_1 and β_2 are varied with the combinations of 10° and 15°. The link lengths, of A_1B, BC, CD and DE as well as angles A_1BC and CDE for each case are tabulated in Table 3.

Based on the reason for selection of Case 4 in Table 2, Case 8 is selected of all the cases in Table 3. In selecting the final design configuration out of Case 4 and Case 8, the force at elbow joint C is considered. Under the condition of constant joint torque needed at joint C, a smaller length of CD would need a larger force to actuate the forearm. This will lead to a large actuator, thus making the structure heavier; also the cost of production would increase. The length of CD is larger in Case 8, hence Case 8 is the final design selected for further consideration.

2.3.2 Design modification based on the singularity condition

A singularity condition arises in the Tyche-arm when the forearm is at 0° (full extension) with respect to the upper arm. At this position joints B, A_2, C and D are collinear. To avoid this the design is modified, by increasing $\angle DCE$ by a small amount of 3°. Due to this change the link lengths of CD and DE change. The modified link lengths are:

CD = 5.731 cm, DE = 19.55, $\angle DCE$ = 8°, $\angle CED$ = 2.39°,
$\angle EDC$ = 169.61.

To prevent the total failure of the Tyche-arm a fault tolerant design is incorporated, by using two linear actuators for activating the parallelogram mechanism. Thus incase of failure of one actuator, the arm would continue functioning, but with reduced efficiency. For the use of linear actuators the link lengths of the parallelogram mechanism had to be changed. Fig. 4 shows the final Tyche-arm. A_2S is the linear actuator and $B_1A_2C_1C$ is the new parallelogram mechanism. The link lengths A_2B_1 and A_2C_1 are calculated based on the fact that the maximum length of the linear actuator (occurring at the full extension of the forearm) should be less than twice the minimum length of the actuator (occurring at full flexion). The link lengths are:

BB_1 = 10.791 cm, B_1C = 5.00 cm , CC_1= 4.029 cm

Fig. 5 shows the solid model of the final Tyche-arm.

3   Copyright © 2002 ARDC by ASME

Table 2. Topological study of the various cases of Tyche-arm, A_2 on A_1C at full flexion

Case	A_1B (cm)	A_1C (cm)	BC (cm)	A_1BC	CD (cm)	CE (cm)	DE (cm)	CDE (degree)
Case 1 $\beta_1=10, \beta_2=10$	0.1138H (19.36)	0.186H (31.62)	0.0764H (12.99)	155	0.0578H (9.83)	0.145H (24.82)	0.0903H (15.36)	160.5
Case2 $\beta_1=10, \beta_2=15$	0.0944H (16.05)	0.186H (31.62)	0.0944H (16.05)	160	0.0387H (6.59)	0.145H (24.82)	0.1384H (23.53)	167.2
Case 3 $\beta_1=15, \beta_2=10$	0.0764H (12.99)	0.186H (31.62)	0.1138H (19.36)	155	0.0471H (8)	0.145H (24.82)	0.099H (16.83)	165
Case 4 $\beta_1=15, \beta_2=15$	0.0473H (8.04)	0.186H (31.62)	0.140H (23.9)	160	0.0245H (4.17)	0.145H (24.82)	0.1205H (20.5)	174

Table 3. Topological study of the various cases of Tyche-arm, $A_1B = A_2B$

Case	A_1B (cm)	A_1C (cm)	BC (cm)	A_1BC	CD (cm)	CE (cm)	DE (cm)	CDE (degree)
Case 5 $\beta_1=10, \beta_2=10$	0.1138H (19.36)	0.186H (31.62)	0.0764H (12.99)	155	0.1138H (19.36)	0.145H (24.82)	0.04635H (7.91)	125.69
Case 6 $\beta_1=10, \beta_2=15$	0.0944H (16.05)	0.186H (31.62)	0.0944H (16.05)	160	0.0944H (16.05)	0.145H (24.82)	0.055H (9.38)	152.72
Case 7 $\beta_1=15, \beta_2=10$	0.0764H (12.99)	0.186H (31.62)	0.1138H (19.36)	155	0.0764H (12.99)	0.145H (24.82)	0.0725H (12.33)	159.37
Case 8 $\beta_1=15, \beta_2=15$	**0.0473H (8.04)**	**0.186H (31.62)**	**0.140H (23.9)**	**160**	**0.0473H (8.05)**	**0.145H (24.82)**	**0.0988H (16.81)**	**172.61**
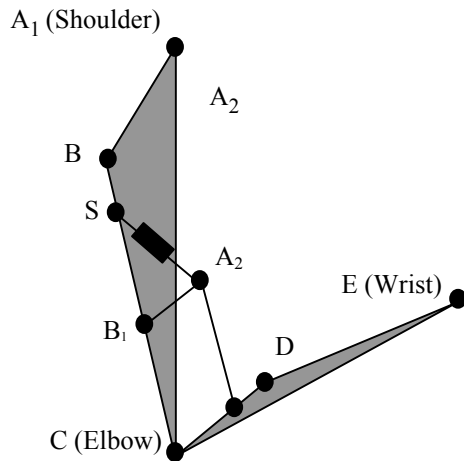
Fig 4. Final Tyche-arm with linear actuator

Fig. 5 Solid model of the Tyche-arm

4   Copyright © 2002 ARDC by ASME
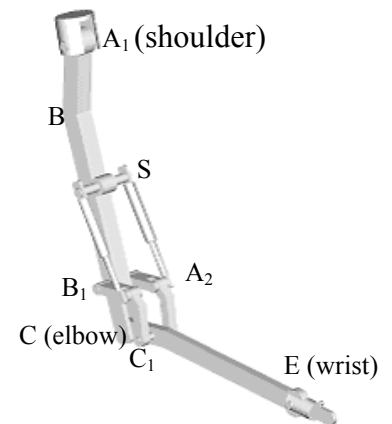
3. KINEMATIC AND DYNAMIC ANALYSES

The kinematic and dynamic analyses of the Tyche-arm are performed using SAM's design, simulation and analysis code. Most of the routine motions of the human arm take place in the plane consisting of the upper arm and the forearm. Hence the 2-D kinematic and dynamic analyses of the Tyche-arm are performed. The Tyche-arm is attached to a frame structure representing the thorax. The link lengths for the frame structure are decided based on the anthropometric data. Fig. 6 shows the SAM model of the Tyche – arm. $F_1F_2F_3 F_4$ is the frame structure representing the thorax. Beam elements, known as links in general, are used to build the Tyche-arm. The upper arm is modeled using four links and the forearm is modeled using three links. All the respective links are constrained relative to each other so that no relative motion takes place among them.

3.1 Simulation of the Tyche-arm

Simulation of the Tyche-arm is performed to acquire the kinematic and dynamic data. The upper arm is fixed with respect to the horizontal and the forearm moves within its range of motion. Five fixed positions of the upper arm are considered, they are:

Case 1: Link A_1C of the Upper arm in the sagittal plane and in a vertical position, the upper arm is in full flexion.

Case 2: Upper arm (A_1C) is at an angle of 45° with the horizontal plane.

Case 3: Upper arm (A_1C) is at an angle of 0° that is upper arm in horizontal position.

Case 4: Upper arm (A_1C) is at an angle of -70° with the horizontal plane.

Case 5: Upper arm (A_1C) is at an angle of -140° with the horizontal plane, that is upper arm in full extension.

To analyze the Tyche – arm for maximum axial link forces and maximum joint torques, the motion of upper limb lifting a weight is considered for simulation. The initial position for simulation is when the thorax, F_1F_2, is bent forward at an angle 45° relative to the horizontal, and the forearm fully extended (0° position with respect to the upper arm). The final position is when the thorax is in upright standing position and the forearm is at its full flexion. A cubic input motion file is selected since the velocity and acceleration are continuous through out the motion. Two input motions, with a simulation time of 4 sec, are defined. The thorax flexion is defined at F_1 joint, which moves from a bent position of 45° with respect to the vertical to a standing position. The range of motion of
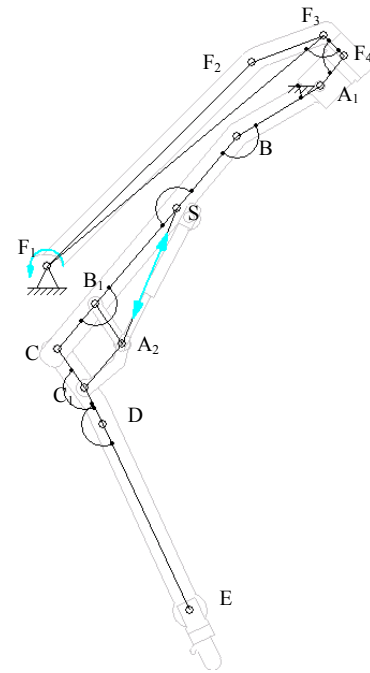

Fig. 6 Model of the Tyche-arm for the kinematic and dynamic

forearm is achieved by defining a compression of 7.34 cm of the link A_2S.

3.2 Kinematic Analysis of the Tyche-arm

Kinematic analysis is carried out with the upper arm in five different positions, discussed above. Both the linear and angular kinematic data of position, velocity and acceleration are obtained

Figs 7a and 7b show the velocity in X and Y direction obtained in Case 1. The velocities start at zero and end at zero since the Tyche-arm starts from rest and stops at standing position. The plots of velocities of the shoulder joint and elbow joint overlap since the upper arm is fixed. The wrist moves closer to the shoulder as the forearm moves from full flexion to full extension. The wrist achieves maximum V_x at 0.6 sec and V_y at 2 sec. A large force is required to begin the motion, since the mechanism is initially at rest. This results in high initial acceleration. The plots of accelerations in X and Y direction (a_x and a_y) with respect to time, obtained in Case 1, are plotted from 0.5 sec to 4 sec in Fig 8a and 8b. Acceleration at 0 sec is tabulated in the plots. As in the case of velocity the acceleration curves of the shoulder and elbow joints overlap.

3.3 Dynamic Analysis of the Tyche-arm

The dynamic analysis is carried out with a payload, varied from 0 to 40 Kgs, at the wrist and on the same five different positions of the upper arm as the kinematics.

5   Copyright © 2002 ARDC by ASME

The masses of the links of the Tyche–arm are applied at the center of gravity of the respective links. The axial forces in the links and joint torques are obtained and plotted with respect to time. A positive force indicates tension and a negative force indicates compression. A positive torque specifies that the torque is acting in clockwise direction and a negative torque implies that the torque acts in anti-clockwise direction. The data obtained from simulation and kinematic and dynamic analyses can be used to choose the proper actuators and controller. The axial forces in the links can be used for further analysis – like FEM.

The plots of axial forces with respect to time, obtained in Case 1, at payloads ranging from 0 Kg to 40 Kg in links SB_1 and B_1C of the upper arm and CC_1 and C_1D of the forearm are illustrated in Figs 9 and 10. It can be concluded from the plots that the axial forces in the links increase as the payload increases. There is an abrupt increase in the axial forces, from 0 sec to 0.5 sec. This is due to the fact that at the initial position the actuator is at its full length and a large force is required to start the compression of the actuator. This force gets transmitted to the beam elements of the upper arm and beam elements of the parallelogram mechanism. A similar trend is seen in the axial forces of the CC_1. The axial forces at 0 sec of such elements are tabulated below the respective plots. Fig. 11 represents the plots of torques at F_1 joint, shoulder joint with respect to time. As seen from the plots the torques increase as the payload increase. The maximum torque at the shoulder occurs at 2 sec. Since at this time the forearm is in horizontal position and that means the payload is at the farthest distance from the shoulder.

4. CONCLUSIONS

An anthropometric robot arm – Tyche-arm, that resembles human arm in size and configuration, has been developed. A pantograph is used as the actuating mechanism. The use of the pantograph generated an amplification factor between the input and the output. Also higher precision and higher payload carrying capacity was obtained. A topological study of various geometries was performed to finalize the link lengths. Other issues like reduced mass of the structure, avoidance of singularity condition and fault tolerant design were also considered. Kinematic and dynamic analyses were performed on the Tyche-arm, with the upper arm fixed at five different positions. A simulation time of 4 sec was taken. The cubic input motion profile was defined for the links. The dynamic analysis was carried out with a payload at the wrist, ranging form 0 Kgs to 40 Kgs with a step of 10 Kgs. The kinematic and dynamic parameters

were obtained and plotted with respect to time. Also there was a sudden increase in the axial forces and torques during the time 0 sec to 0.5 sec. This was due to inertial effect of the links and also due to action of the actuator.

REFERENCES

[1] Fukuda, T., Michnelini, R., Potkonjak, S., Tzafestas, S., Valavanis, K. and Vukobratovic, M., "How far away is 'Artificial Man'?" *IEEE Robotics and Automation*, March 2001, pp. 66-73.

[2] Giszter, S. F., Moxon, K.A. and Chapin, J.K., "A Neurobiological Perspective on Humanoid Robot Design", *IEEE Intelligent Systems*, 2000, pp. 64-69.

[3] Kirschner, S.K and Miller, C., "*SDR – 3*", Popular Science, September, pp. 5.

[4] Hayden, T., 2001, *"The Age of Robot,"* U.S. News and World Report, April, pp. 44-50.

[5] Kawamura, K., Peters, R.A., Wilkes, D.M., Alford, W.A., Rogers, T.E., " ISAC: Foundations in Human-Humanoid Interaction", *IEEE Intelligent Systems*, 2000, pp. 38 - 45.

[6] Ambrose, R.O., Aldridge, H., Askew, R.S., Burridge, R.R, Bluethmann, W., Myron, D., Lovchik, C., Magruder, D. and Fredrick, R., "Robonaut: NASA's Space Humanoid", *IEEE Intelligent Systems*, 2000, pp. 57-63.

[7] Berns, K., Asfour, T., and Dillmann R., "ARAMR–An Anthropomorphic Arm for Humanoid Service Robot," *Proceedings of the IEEE International Conference on Robotics and Automation*, 1999, pp. 702- 707.

[8] Yuji, M., 1990, "Development of an Anthropomorphic Robot Arm (Mark-2)", IEEE *Proceedings of the International Workshop on Intelligent Motion Control*, vol. 1, pp. 389-394.

[9] Nakamura, Y. and Yamane, K., "Dynamics Computation of Structure − Varying Kinematic Chains and Its Application to Human Figures", *IEEE Transactions on Robotics and Automation,* 2000, pp.124 – 133.

[10] Nielsen, J. and Roth, B., "On the Kinematic Analysis of Robotic Mechanisms", *The*

6   Copyright © 2002 ARDC by ASME

International Journal of Robotics Research, 1999, pp. 1147 – 1160.

[11]   Chirikjian, G.S., "Kinematic Synthesis of Mechanisms and Robotic Manipulators with Binary Actuators", *ASME Journal of Mechanical Design,* 1995, pp. 573 – 580.

[12]   Lee, M.K., " Kinematic and Dynamic Analysis of A Double Parallel Manipulator for Enlarging Workspace and Avoiding Singularities", *IEEE Transactions on Robotics and Automation,* 1999, pp. 1024 – 1034.

[13]   Cheng, L.P. and Kazerounian, K., 2000, "Study and Enumeration of Singular Configurations for the Kinematic Model of Human Arm", *IEEE Proceedings of the 26th Annual Northeast Bioengineering Conference*, pp. 3-4.

[14]   I.A Kapandji, The Physiology of The Joints, Volume 1, Upper Limb, Churchill Living Stone, 1970.

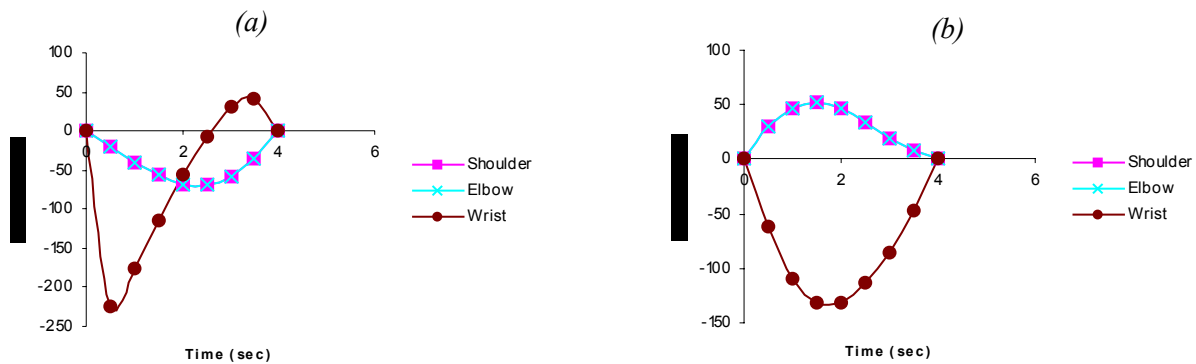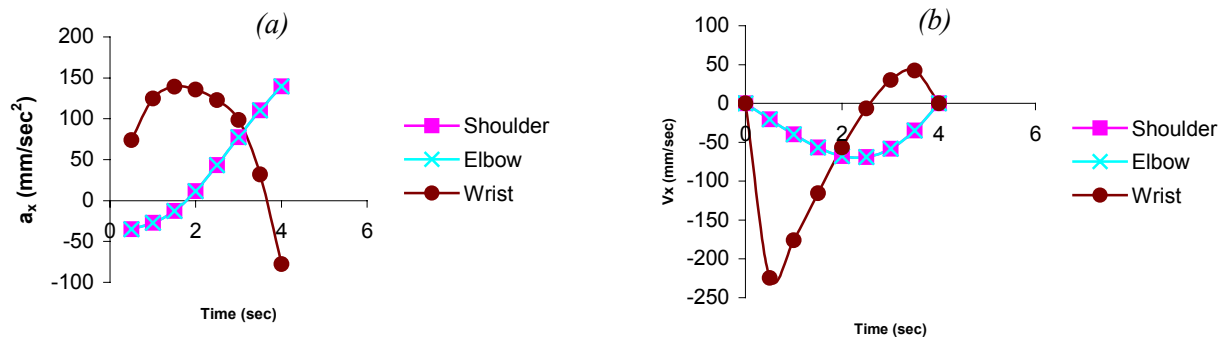[15]   Winter, D.A, 1990 – Biomechanics and Motor Control of Human Movement, John Wiley and Sons,   Inc.

Fig. 7 Velocity of joints in Case 1 *(a)* Velocity in X direction *(b)* Velocity in Y

Joint	Shoulder	Elbow	Wrist
Accl at t=0(mm/sec^2)	-44.904	-44.904	-44.904

Joint	Shoulder	Elbow	Wrist
Accl at t=0(mm/sec^2)	-44.904	-44.904	-44.904

Fig.8 Acceleration of joints in Case 1 *(a)* Acceleration in X direction *(b)* Acceleration in Y direction
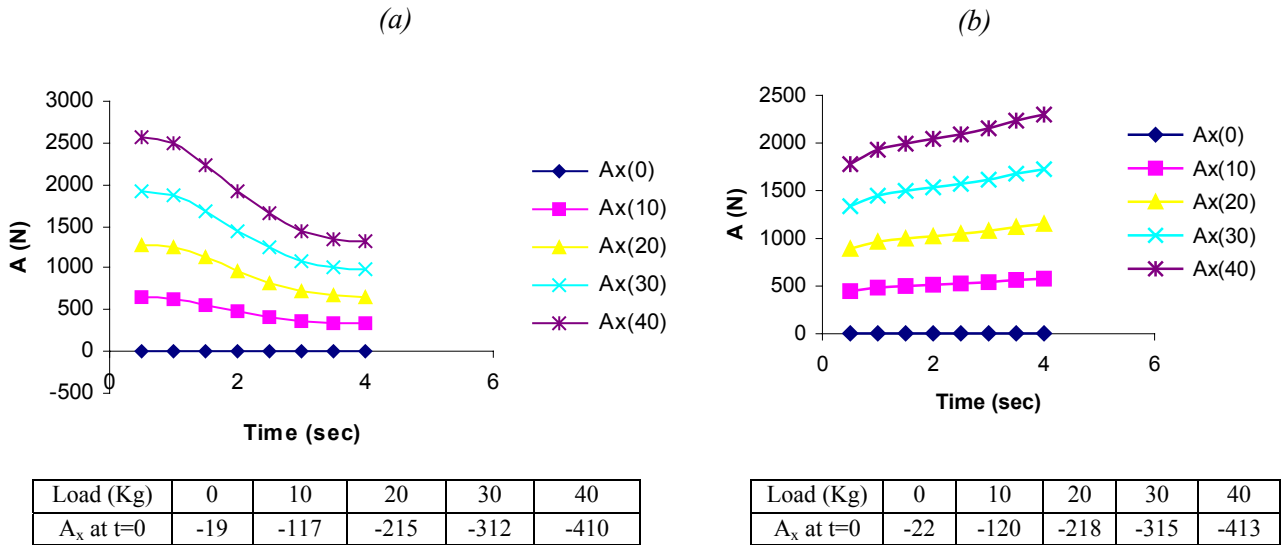
7   Copyright © 2002 ARDC by ASME

(a) | *(b)*

Load (Kg)	0	10	20	30	40
A_x at t=0	-19	-117	-215	-312	-410

Load (Kg)	0	10	20	30	40
A_x at t=0	-22	-120	-218	-315	-413

Fig. 9 Axial Forces in Upper arm in Case 1 *(a)* Axial forces in SB_1 *(b)* Axial forces in B_1C

(a) | *(b)*

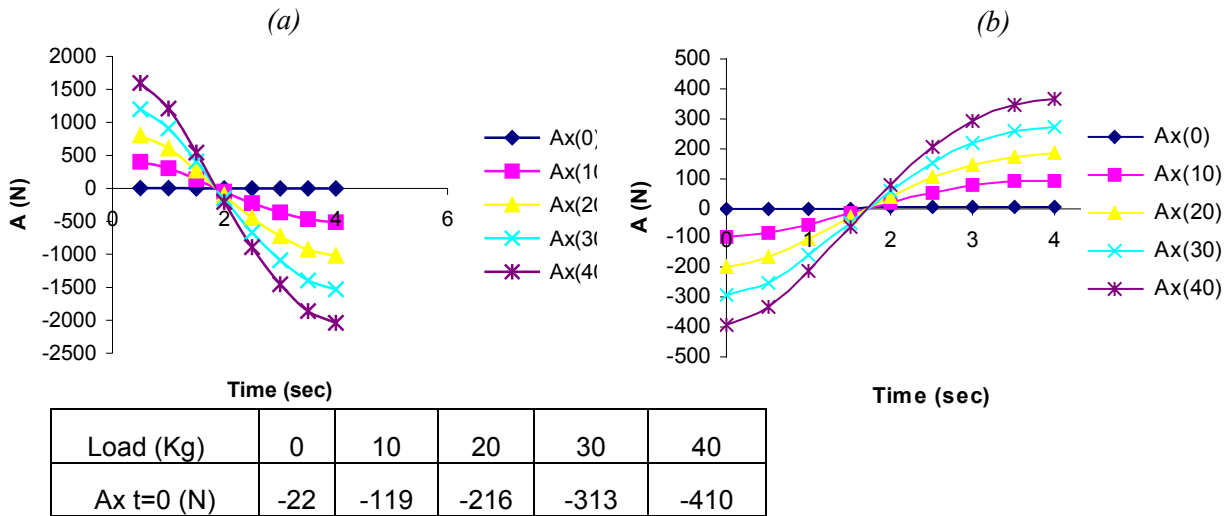| Load (Kg)	0	10	20	30	40
Ax t=0 (N)	-22	-119	-216	-313	-410

Fig. 10 Axial Forces in Forearm in Case 1 *(a)* Axial forces in CC_1 *(b)* Axial forces in C_1D
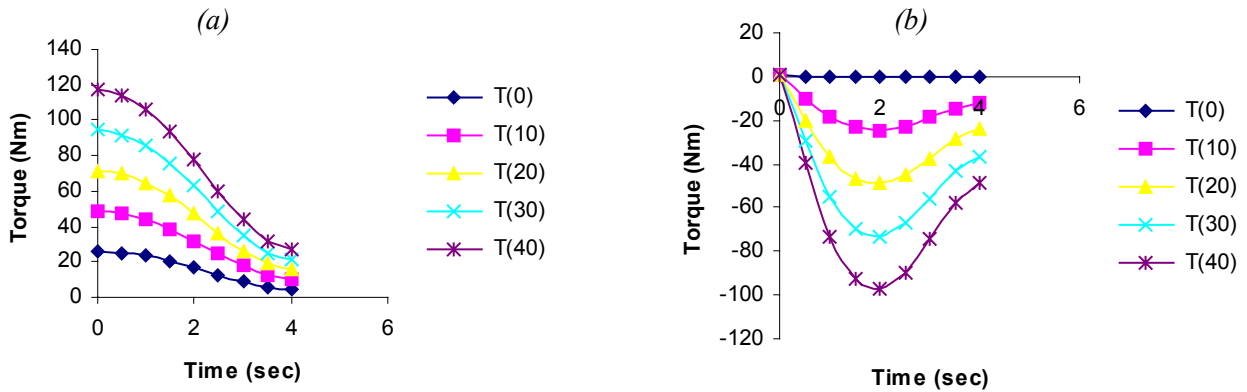

(a) | *(b)*

Fig. 11 Torques at joints in Case 1; *(a)* Torques at F_1 joint *(b)* Torques at shoulder joint

8   Copyright © 2002 ARDC by ASME